

Comparative Analysis of Syntenic Genes in Grass Genomes Reveals Accelerated Rates of Gene Structure and Coding Sequence Evolution in Polyploid Wheat¹[W][OA]

Eduard D. Akhunov^{2*}, Sunish Sehgal², Hanquan Liang, Shichen Wang, Alina R. Akhunova, Gaganpreet Kaur, Wanlong Li, Kerrie L. Forrest, Deven See, Hana Šimková, Yaqin Ma, Matthew J. Hayden, Mingcheng Luo, Justin D. Faris, Jaroslav Doležel, and Bikram S. Gill

Department of Plant Pathology (E.D.A., S.S., H.L., S.W., A.R.A., G.K., B.S.G.) and Integrated Genomics Facility, (H.L., A.R.A.), Kansas State University, Manhattan, Kansas 66506; Plant Science, Biology, and Microbiology, South Dakota State University, Brookings, South Dakota 57007 (W.L.); Department of Primary Industries Victoria, Victorian AgriBiosciences Center, Bundoora, Victoria 3083, Australia (K.L.F., M.J.H.); United States Department of Agriculture-Agricultural Research Service, Western Regional Small Grains Genotyping Laboratory, Washington State University, Pullman, Washington 99164 (D.S.); Centre of the Region Haná for Biotechnological and Agricultural Research, Institute of Experimental Botany, CZ-77200 Olomouc, Czech Republic (H.Š., J.D.); Department of Plant Sciences, University of California, Davis, California 95616 (Y.M., M.L.); Department of Botany and Plant Sciences, University of California, Riverside, California 92521 (Y.M.); United States Department of Agriculture-Agricultural Research Service, Northern Crop Science Laboratory, Fargo, North Dakota 58102-2765 (J.D.F.); and King Abdulaziz University, Faculty of Science, Genomics and Biotechnology Section, Department of Biological Sciences, Jeddah 21589, Saudi Arabia (B.S.G.)

Cycles of whole-genome duplication (WGD) and diploidization are hallmarks of eukaryotic genome evolution and speciation. Polyploid wheat (*Triticum aestivum*) has had a massive increase in genome size largely due to recent WGDs. How these processes may impact the dynamics of gene evolution was studied by comparing the patterns of gene structure changes, alternative splicing (AS), and codon substitution rates among wheat and model grass genomes. In orthologous gene sets, significantly more acquired and lost exonic sequences were detected in wheat than in model grasses. In wheat, 35% of these gene structure rearrangements resulted in frame-shift mutations and premature termination codons. An increased codon mutation rate in the wheat lineage compared with *Brachypodium distachyon* was found for 17% of orthologs. The discovery of premature termination codons in 38% of expressed genes was consistent with ongoing pseudogenization of the wheat genome. The rates of AS within the individual wheat subgenomes (21%–25%) were similar to diploid plants. However, we uncovered a high level of AS pattern divergence between the duplicated homeologous copies of genes. Our results are consistent with the accelerated accumulation of AS isoforms, nonsynonymous mutations, and gene structure rearrangements in the wheat lineage, likely due to genetic redundancy created by WGDs. Whereas these processes mostly contribute to the degeneration of a duplicated genome and its diploidization, they have the potential to facilitate the origin of new functional variations, which, upon selection in the evolutionary lineage, may play an important role in the origin of novel traits.

¹ This work was supported by the U.S. Department of Agriculture National Institute of Food and Agriculture (grant nos. 2006-35604-17248 to B.S.G., 2008-35300-04588 to B.S.G., and CRIS0219050 to E.D.A.), by the Kansas Wheat Commission (to E.D.A.), by the Grains Research and Development Corporation of Australia (to M.J.H.), by the Ministry of Education, Youth, and Sports of the Czech Republic and the European Regional Development Fund (Operational Programme Research and Development for Innovations grant no. ED0007/01/01 to H.Š. and J.D.), and by Kansas Agricultural Experiment Station grants to the Wheat Genetics Resources Center (to B.S.G.) and the Integrated Genomics Facility (to A.R.A.).

² These authors contributed equally to the article.

* Corresponding author; e-mail eakhunov@ksu.edu.

The author responsible for distribution of materials integral to the findings presented in this article in accordance with the policy described in the Instructions for Authors (www.plantphysiol.org) is: Eduard D. Akhunov (eakhunov@ksu.edu).

[W] The online version of this article contains Web-only data.

[OA] Open Access articles can be viewed online without a subscription.

www.plantphysiol.org/cgi/doi/10.1104/pp.112.205161

The evolution of protein-coding sequences, gene exon-intron structure, and alternative splicing (AS) define the diversity of proteome structure and function (Koonin and Wolf, 2010). Multiple studies performed mostly on diploid species or ancient polyploids suggested that gene duplication plays a major role in coding sequence evolution (Ohno, 1970; Lynch and Conery, 2000; Fan et al., 2008; Roux and Robinson-Rechavi, 2011). According to the hypothesis of Ohno (1970), gene duplications lead to relaxed selection, which allows duplicated genes to accumulate mutations. The evolutionary fate of redundant genes is defined by selection that can drive beneficial alleles to fixation, resulting in the creation of novel gene functions through the processes of neofunctionalization and subfunctionalization (Ohno, 1970; Hughes, 1994; Force et al., 1999). Alternatively, genes can become nonfunctional and eventually lost from evolutionary lineages.

The discovery of paleopolyploidy in most of the analyzed plant genomes has highlighted the importance of whole-genome duplication (WGD) in the evolutionary success of flowering plants (Paterson et al., 2003; Soltis et al., 2008; Van de Peer et al., 2009). In ancient polyploids, it was shown that retained copies of duplicated genes are under selective constraint, as estimated from the distribution of the ratio of nonsynonymous to synonymous mutations (d_N/d_S) values (Lin et al., 2010), or they show a high level of connectivity in gene networks (Severin et al., 2011). In maize (*Zea mays*), the probability of gene loss was associated with the reduced contribution of a duplicated copy to the total level of gene expression (Schnable et al., 2011). These facts are consistent with the “gene balance hypothesis,” suggesting that dosage-sensitive genes are very likely to be retained after WGD (Birchler and Veitia, 2007; Freeling, 2009). While these studies have demonstrated the long-term consequences of polyploidization, the impact of recent WGD on genome coding potential is still not fully understood. The analysis of artificially synthesized polyploid plants suggests that WGD results in “genomic shock” accompanied by structural rearrangements (Kashkush et al., 2002; Gaeta et al., 2009), activation of transposons (Kashkush et al., 2003), expression changes (Pumphrey et al., 2009; Akhunova et al., 2010), and epigenetic modifications (Chen et al., 2008; Ni et al., 2009). These processes can become a source of new transgressive variation and provide the molecular basis for functional evolution (Osborn et al., 2003; Comai, 2005; Chen, 2007). Among plant species, wheat (*Triticum aestivum*) provides a unique opportunity to study early phases of duplicated gene evolution after WGD, the impact of increased genome size on the evolutionary dynamic of gene space, and understand how these processes shaped the coding potential of the wheat genome.

The hexaploid wheat genome (comprised of about 16,000 Mb) resulted from the union of three diploid grass species. The first hybridization event, which resulted in the origin of tetraploid wheat, occurred 0.36 to 0.5 million years ago (Dvorák and Zhang, 1990; Dvorák et al., 1993; Huang et al., 2002; Dvorak and Akhunov, 2005; Chalupska et al., 2008), and the second hybridization event, which resulted in the origin of hexaploid bread wheat, occurred about 8,000 years ago (Kihara, 1944; McFadden and Sears, 1944, 1946; Nesbitt and Samuel, 1996). Early analyses of EST maps show that about 20% of wheat genes are interchromosomally duplicated (Akhunov et al., 2003; Qi et al., 2004). Comparative analysis of model grass genomes (International Rice Genome Sequencing Project, 2005; Paterson et al., 2009; Schnable et al., 2009; International Brachypodium Initiative, 2010) revealed a more detailed picture of wheat genome structure evolution involving segmental duplications, chromosome inversions, translocations, and small-scale structural rearrangements (Akhunov et al., 2003; Gu et al., 2004, 2006; Salse et al., 2008; Choulet et al., 2010; Devos, 2010; Mayer et al., 2011; Wicker et al.,

2011). These studies demonstrated an acceleration of genome structure evolution in wheat, which also had an impact on the evolution of the gene repertoire (Akhunov et al., 2007; Salse et al., 2008; Massa et al., 2011). However, the impact of these processes on the dynamics of gene structure evolution in the wheat genome has not been thoroughly investigated. The evolution of gene structure in eukaryotes was previously shown to be associated with exon shuffling, retroposition, transposon recruitment, or gene fusion (Long et al., 2003). Studies performed in plant species with small genomes, such as rice (*Oryza sativa*; Wang et al., 2006; Fan et al., 2008) and poplar (*Populus* spp.; Zhu et al., 2009), revealed the importance of exon shuffling and retroposition in diversification of the coding potential of plant genomes. While recent studies showed evidence of transposon recruitment in the wheat genome (Akhunov et al., 2007; Wicker et al., 2011), the role of other mechanisms in gene structure evolution was not characterized.

AS is commonly used by eukaryotic organisms to enhance proteome diversity and regulate transcript abundance (Ast, 2004; Reddy, 2007). The true scale of AS in plant genomes began to emerge only recently with the availability of deep RNA sequencing data. These studies have predicted that more than 20% of genes in maize and rice, and more than 40% in *Arabidopsis* (*Arabidopsis thaliana*), undergo AS (Barbazuk et al., 2008; Filichkin et al., 2010; Zhang et al., 2010). In wheat, only a limited number of genes have been characterized for AS events (Båga et al., 1999; Terashima and Takumi, 2009), and the impact of WGD on AS patterns on a genome-wide scale remains unknown.

Here, we performed intraspecies and interspecies comparative analyses of the wheat genome and model grass genomes to investigate the dynamics of gene structure, AS, and coding sequence evolution in the wheat lineage. As part of the International Wheat Genome Sequencing Consortium effort (www.wheatgenome.org), we developed a high-density syntenic map of wheat chromosome 3A (827 Mb) using 9.2× coverage sequence data generated with 454 sequencing technology. These data were combined with publicly accessible wheat genomic sequences from the National Center for Biotechnology Information (NCBI) database to analyze the evolutionary dynamic of gene structure in the polyploid wheat genome and to describe homeolog-specific patterns of AS. Developed gene models were annotated and used to reveal genes that had lost their function due to the accumulation of premature termination codons (PTCs) and genes whose codons accumulate nonsynonymous mutations at accelerated rates. Comparative analysis of orthologous gene sets between the syntenic regions of the model grass genomes and wheat was performed to estimate the rate, and to understand the molecular mechanisms, of gene structure evolution in wheat. The gene structure and patterns of AS were compared between homeologous genes to assess the extent of

functional differentiation between the wheat sub-genomes.

RESULTS

Wheat Chromosome 3A Assembly

Out of 25.3 million 454 reads (7.65 Gb), 16.9 million (5.2 Gb) were assembled into 240,121 large contigs (LC; 500 bp or greater) with a total length of 331 Mb, representing 40% of the physical length of chromosome 3A (Supplemental Table S1). The remaining 32% of reads were not included in the assembly due to having only partial overlap with contigs (588 Mb), absence of overlap with any other reads (335 Mb), high copy number (715 Mb), and/or artifacts such as chimeric sequences (842 Mb). The reduced level of chromosome coverage comes from the presence of highly abundant repetitive elements assembled into short contigs with deep sequence coverage (Supplemental Fig. S1). The estimate of N50 (the weighted median value such that 50% of the assembly is contained in contigs equal to or larger than this value) for LC was 1,692 bp (Table I). Using paired-end sequence reads, nearly 60% (195 Mb) of LC were assembled into 38,036 scaffolds with an N50 size of 6,013 bp (Table I) and a total gap length of 17 Mb. The final data set included both scaffolds (2,000 bp or greater) and LC (not included into the scaffolds) with a total length of 348 Mb (Table I).

The fraction of targeted chromosomal arms in flow-sorted material was 86% to 92% (Supplemental Table S2). We confirmed these estimates by comparing LC sequences with the sequences of single-copy wheat ESTs mapped to the deletion bins on wheat chromosome 3 (wheat.pw.usda.gov/wEST). A total of 374 ESTs were selected for this analysis, of which 87% had significant BLASTN hits with chromosome 3A contigs and scaffolds (alignment length, 100 or greater; identity, 90% or greater). Comparison of 5,288 ESTs mapped to wheat chromosomes other than chromosome 3 showed only 705 significant BLASTN hits, suggesting that contamination of the flow-sorted material was less than 13%. The distribution of alignment depth in the contig assemblies was consistent with genome coverage of approximately 7× to 8× (Supplemental Fig. S2). This coverage is slightly lower than the expected 9.3× coverage and can be, at least partially, explained by contamination from other wheat chromosomes.

There is a possibility that the DNA contamination would impact the results of downstream analyses due to the presence of duplicated genes on other chromosomes, including homeologous genes on chromosomes 3B and 3D. The divergence of these genes from true orthologous genes may bias our estimates of the rates of gene evolution. Assuming that the fraction of chromosome 3A gene homologs located elsewhere in the wheat genome is about 14.7% (Supplemental Materials and Methods S1), we estimated that, in our data set, about 1.9% of coding sequences could be mistaken for true chromosome 3A genes. However, we expect that this bias will likely be low due to the 100-fold lower level of coverage (0.07×) achieved for the contaminating fraction (13%) of the wheat genome in our sample compared with the 7× coverage obtained for chromosome 3A (Supplemental Material). The low level of coverage obtained for contaminating DNA should reduce the contribution of contaminating reads to consensus sequences of the chromosome 3A contigs and the fraction of contaminating gene sequences assembled into contigs longer than 500 bp (Supplemental Material).

The impact of flow-sorted chromosome contamination on evolutionary inferences should also be reduced by selecting syntenic genes sharing positional orthology among cereal genomes. However, this approach may also introduce bias in our evolutionary rate estimates, because it has been shown that positionally conserved genes may be under stronger selection constraint (Notebaart et al., 2005). In contrast, transposed orthologous genes were shown to evolve faster (Han et al., 2009). In our case, gene selection using positional orthology will most likely result in an underestimation of evolutionary changes in the wheat genome, thereby producing more conservative estimates.

The accuracy of chromosome 3A sequence assembly was assessed by comparing masked contigs and scaffolds with previously sequenced bacterial artificial chromosome (BAC) clones from the wheat chromosome 3A BAC library. A total of 17 BAC clones (total length of 2,094,375 bp), spanning the region of wheat chromosome 3A homeologous to the fusarium head blight resistance gene (*Fhb1*) locus on chromosome 3B, were used in the comparison (Supplemental Table S3). The error rate estimated from this analysis was 0.07%, caused by small-scale insertions/deletions in the

Table I. The chromosome 3A assembly statistics

Parameter	Large Contigs (500 bp or Greater)	Scaffolds (2,000 bp or Greater)	Large Contigs (500 bp or Greater) and Scaffolds
No. of contigs/scaffolds	240,121	38,036	213,660
No. of bases	330,997,554	195,458,009	348,362,074
Average size (bp)	1,378	5,138	1,630
N50 size (bp)	1,692	6,013	2,689
Largest size (bp)	43,015	69,248	69,248
Ns in gaps (bp)	–	17,125,261	17,125,261

regions of homopolymeric bases (the most common source of error in 454 sequence data, followed by single base errors). This result also suggests that the proportion of errors due to contamination with homeologous chromosomes 3B and 3D should be relatively low in our sample. Chromosome 3A assemblies covered about 85% of the repeat-masked portion of the wheat chromosome 3A BAC clones.

Syntenic Gene Order

The chromosome 3A contigs and scaffolds were ordered based on the syntenic relationships with *Brachypodium distachyon*, rice, and sorghum (*Sorghum bicolor*) using a strategy similar to that used by Mayer et al. (2011) and described in detail in the Supplemental Material. The conserved syntenic regions of the three model grass genomes were used to recreate a hypothetical order of genes along wheat chromosome 3A (Fig. 1A). A total of 3,646 chromosome 3A contigs/scaffolds were ordered to construct the chromosome 3A syntenic gene order (SGO) map (Supplemental Table S8). The order of genes inferred using the grass genome synteny was largely consistent with the recombination-based single-nucleotide polymorphism (SNP) genetic map of *Aegilops tauschii*, the diploid D-genome progenitor of polyploid wheat (Luo et al., 2009; Supplemental Fig. S7). The SGO map, based on conserved orthologous gene sets, provides a robust framework for investigating the evolutionary relationships of 3A with other cereal genomes (Fig. 1) and among wheat chromosomes (Supplemental Table S9; Supplemental Fig. S8). In addition, the selection of syntenic genes reduces the impact of flow-sorted chromosome contamination on evolutionary inferences made in our study.

Comparison of bin-mapped wheat ESTs with the genes from the 3A SGO map revealed 249 unique BLASTN hits detecting 10 segmental duplications

involving chromosome 3A and other groups of wheat chromosomes (Supplemental Table S9). There were three duplicated blocks on the chromosome combination w3-w1, two on w3-w2, three on w3-w5, and two on w3-w7 (Supplemental Fig. S8). Five of the detected duplications are new, and five have been described previously (Salse et al., 2008). Except for the ancient w3-w1 duplication shared between wheat and rice, all the duplicated regions occurred in the wheat lineage. All were shared among the three homeologous chromosomes of each group, suggesting that these duplication events originated before the split of diploid wheat ancestors.

We also used the SGO map to detect the centromeric region of chromosome 3A. We identified 510 SGO contigs/scaffolds mapped to the 3AS arm and 858 SGO contigs/scaffolds mapped to the 3AL arm. Eighty-two contigs and scaffolds, starting with SGO1163 and ending with SGO1394, mapped to either of the chromosome arms and spanned 10 Mb on the homeologous region of rice chromosome 1 (Supplemental Table S10). We further refined the location of the centromere using wheat ESTs (BF485348, BE637878, BG313557, and BE404580) previously used for comparative analyses of centromere locations in wheat, rice, and *B. distachyon* (Qi et al., 2010). Based on this analysis, the location of the centromere on wheat chromosome 3A was further reduced to a region flanked by SGO1221 and SGO1367, which corresponds to a homeologous 7.7-Mb region in the rice genome (Fig. 1B).

Evidence-Based Gene Prediction

Evidence-based annotation of gene exon-intron structure was performed using contig assemblies, including chromosome 3A contigs generated in our study and 371 BAC contig sequences available in the NCBI database (Supplemental Table S11). The latter

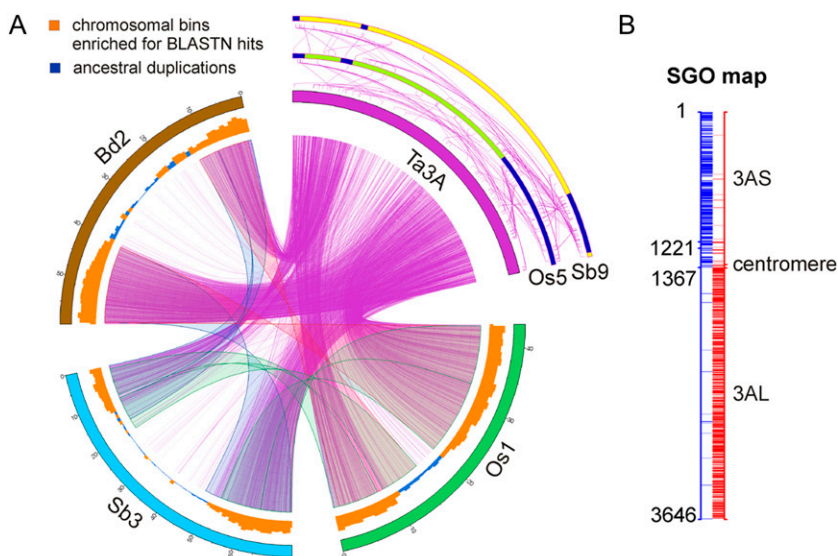


Figure 1. Comparative analysis between wheat chromosome 3A and the sequenced genomes of *B. distachyon*, rice, and sorghum. A, Comparison of the wheat chromosome 3A SGO map (Ta3A) with sorghum chromosomes 3 and 9 (Sb3 and Sb9), rice chromosomes 1 and 5 (Os1 and Os5), and *B. distachyon* chromosome 2 (Bd2). Ancestral chromosome duplications predating the divergence of wheat, rice, *B. distachyon*, and sorghum are colored in blue; chromosomal bins enriched for BLASTN hits with chromosome 3A contigs are colored in orange. B, Location of the wheat chromosome 3A centromere was inferred by BLASTN comparison of SGO with the 454 reads generated for flow-sorted 3AS and 3AL chromosomal arms. The locations of two chromosome 3A contigs on the SGO map (SGO1221 and SGO1367) showing similarity to previously mapped EST markers flanking the wheat centromere are shown.

data set included 12 and 24 contigs originating from chromosome 3B (Choulet et al., 2010) and 3D (Bartoš et al., 2012), respectively, combined with contigs distributed across the wheat genome. The total length of the BAC contigs was 50.3 Mb, out of which 17.9 and 1.6 Mb represented sequences from wheat chromosome 3B (Choulet et al., 2010) and 3D (Bartoš et al., 2012), respectively. The length of the wheat contigs varied from 20 kb to 3.1 Mb.

For predicting gene models in the wheat genome, we used only those transcript sequences (Supplemental Table S12) that met the similarity threshold (98.5%) established for separating homeologs (for details, see "Materials and Methods"). Assessment of previously published data for the distribution of intergenomic sequence similarity levels in the genic regions of the wheat genome (Akhunov et al., 2010) suggests that this threshold can separate wheat homeologs with 94.3% accuracy (Supplemental Materials and Methods S1). The remaining 5.7% of predicted genes could result from erroneously aligned transcripts caused by low levels of intergenomic divergence. A total of 6,366 complete or partial gene structures were predicted on chromosome 3A contigs (Table II). The average sizes of predicted introns (131 bp) and exons (171 bp) were also similar to previous estimates obtained by BAC sequencing (Choulet et al., 2010), suggesting that predictions of intron-exon structure using chromosome 3A assemblies do not result in biased estimates. By aligning 31,292 transcripts to wheat BAC contigs distributed across the wheat genome, we detected 1,049 genes, out of which 391 and 91 were predicted on the wheat chromosome 3B and 3D contigs, respectively (Table II).

AS in the Polyploid Wheat Genome

AS is one of the major mechanisms used by eukaryotes to increase transcriptome and proteome diversity. We used extensive transcriptome sequence data assembled into homeolog-specific transcripts to gain insights into the patterns of AS in the polyploid wheat genome (Table III; Supplemental Fig. S9). The use of 454 sequence data obtained from normalized complementary DNA (cDNA) libraries should ensure deep sampling of unique alternatively spliced transcripts in the genome. More than 24% of genes predicted on wheat chromosomes 3A, 3B, and 3D showed evidence of AS (Table III). Only a slightly lower fraction of AS

events (21%) was predicted in a sample of BAC clones distributed across the wheat genome, suggesting that trends observed on wheat chromosomes 3A, 3B, and 3D do not depart dramatically from that of the whole genome.

Consistent with observations in other plant systems (Barbazuk et al., 2008; Lu et al., 2010; Marquez et al., 2012), the major classes of AS variants in the wheat genome were retained intron (RI; 30%–37%) and alternative acceptor (AA; 26%–43%) variants, followed by alternative donor (AD; 22%–28%) and skipped exon (SE; 4%–7%) spliced variants. In the majority (91%) of cases, intron retention in wheat resulted in PTCs.

Evolution of AS Forms

Although previous studies demonstrated that, in most cases, duplicated copies of genes in polyploid wheat are expressed (Nomura et al., 2005; Bottley and Koebner, 2008; Akhunova et al., 2010), the degree of AS pattern similarity between them remains unknown. We estimated AS divergence using a set of 86 and 20 homeologous gene pairs identified between wheat chromosomes 3A and 3B (Choulet et al., 2010) and 3A and 3D (Bartoš et al., 2012), respectively. Even considering a 5.7% false-positive rate in homeologous transcript alignment, the wheat genomes showed substantial levels of AS divergence. Among identified gene pairs, 33 (37%) and eight (40%) showed evidence of AS in the 3A-3B and 3A-3D genome comparisons, respectively (Table IV; Supplemental Table S13). We found that 39%, 28%, 28%, and 5% of AS events in the 3A-3B comparison, and 32%, 39%, 21%, and 7% of AS events in the 3A-3D comparison, belong to RI, AD, AA, and SE types, respectively (Table IV). The proportion of the AS events different between the homeologous gene pairs in the 3A-3B and 3A-3D comparisons was 42% and 61%, respectively. The divergence between the wheat genomes was highest for RI events and smallest for AD events.

Previously, it was shown that the depth of sequence data impacts the probability of recovering AS events (Barbazuk et al., 2008). To assess the possibility of this type of bias in the estimation of AS divergence between homeologs, we compared the proportion of AS events between shared and homeolog-specific AS isoforms that are supported by a single EST/transcript. We found that these proportions among homeolog-

Table II. Summary of gene prediction using the PASA pipeline

Parameter	3A	3B ^a	3D ^a	Whole-Genome Sample ^b
Total transcript sequences	1,097,184	8,945	1,138	31,292
No. of transcripts with any alignment	268,190	6,197	1,072	31,118
Valid GMAP alignments	60,301	2,715	531	22,006
No. of subclusters (genes)	6,366	391	91	1,049

^aSequences of BAC contigs from wheat chromosomes 3B (Choulet et al., 2010) and 3D (Bartoš et al., 2012). ^bSequences of BAC contigs downloaded from the NCBI database.

Table III. Analysis of AS in the wheat genome

Events	454 Assemblies			Whole-Genome Sample
	3A	3B	3D	
Involved in AS	1,912 (24.8)	118 (24.8)	27 (24.3)	235 (20.9)
AA	686 (35.9)	51 (43.2)	7 (25.9)	66 (28.1)
AD	447 (23.4)	33 (28.0)	6 (22.2)	62 (26.4)
RI	636 (33.3)	44 (37.3)	8 (29.6)	84 (35.7)
SE	117 (6.1)	5 (4.2)	2 (7.4)	15 (6.4)

specific (7%) and shared (5%) AS events were similar, suggesting that the depth of sequencing did not have significant impact on our estimates of AS divergence between the wheat genomes.

Next, we compared the level of AS conservation observed in our study with previous estimates of AS conservation between rice and Arabidopsis (Wang and Brendel, 2006). Using a similar approach applied to 643 wheat-rice orthologous gene pairs, we identified 2,292 introns. Out of these gene pairs, 264 and 239 were alternatively spliced in wheat and rice, respectively. Among the 232 conserved introns identified in these genes, only 19 (8%) showed the same type of AS in both rice and wheat. Intron retention was the most conserved type of AS event between rice and wheat, with only 5% of the genes showing intron retention in both rice and wheat (Table V). This estimate is two times lower than that obtained for Arabidopsis and rice (Wang and Brendel, 2006).

Evolution of Gene Structure

To investigate the dynamics of gene structure evolution in the polyploid wheat genome, we compared protein sequences of orthologous genes between wheat, *B. distachyon*, and rice (Fig. 2A). A total of 1,059 orthologous gene pairs between wheat chromosome 3A and rice, and 839 orthologous gene pairs between wheat chromosome 3A and *B. distachyon*, were analyzed (Fig. 2B; Supplemental Table S14). In addition, patterns of gene structure conservation and divergence were characterized between homeologous genes on wheat chromosomes 3A, 3B, and 3D and among orthologous gene sets identified in a sample of sequenced BAC clones distributed across the wheat genome and model genomes. Of 958 genes that were predicted in the wheat BAC clones, we identified 169 rice and 194 *B. distachyon* orthologs. Of the 391 genes predicted in

wheat chromosome 3B BAC contigs, 86 had homeologous copies on wheat chromosome 3A, and out of 91 genes predicted in the chromosome 3D BAC contigs, 20 had duplicates on wheat chromosome 3A.

The proportion of lost and acquired exonic sequences was higher in wheat-rice and wheat-*B. distachyon* comparisons than in rice-*B. distachyon* comparisons (Fig. 2B). This trend was consistent among all three sets of orthologous genes predicted in wheat chromosomes 3A, 3B, and 3D and a sample of BAC clones distributed across the wheat genome. There was an average of 2.5 times fewer acquired exons and five times fewer lost exons discovered by comparing rice with *B. distachyon* than by comparing wheat and either of the two model genomes. Consistent with this observation, the proportion of conserved exons between rice and to *B. distachyon* was from 25% to 37% higher than that in wheat-rice and wheat-*B. distachyon* comparisons (Fig. 2B). The distribution of exon loss and acquisition events along the wheat genes was similar. The means of relative locations of exon acquisition and loss events along the coding sequence (from 0 to 1), estimated according to Fawcett et al. (2012) by dividing the distance of an event from the 5' end by the total length of coding sequence, were 0.43 and 0.38, respectively.

We identified 68 genes that contained 130 acquired exons (length of 30 bp or greater) specific to the wheat lineage (Supplemental Table S15). In a randomly selected sample of 36 acquired exons, 72% were confirmed by reverse transcription PCR (Supplemental Table S16). Searches of the NCBI database revealed that only 17 exons had significant BLASTN hits to coding sequences (E value < $1e^{-10}$), suggesting that about 13% of genes in the wheat genome could have evolved by exon shuffling. Most of these exons were found only in the Triticeae lineage and showed similarity to barley (*Hordeum vulgare*) or wheat ESTs/cDNAs. Nine of the acquired exons were similar to

Table IV. Comparison of AS types between duplicated gene pairs on homeologous chromosomes 3A, 3B, and 3D

AS Types	3A-3B Comparison			3A-3D Comparison		
	Count in 3B	Count in 3A	Different AS Events	Count in 3D	Count in 3A	Different AS Events
AD	14	10	5	8	3	4
AA	15	9	11	1	5	4
RI	19	14	19	6	3	9
SE	3	1	1	1	1	0

Table V. Conservation of AS events in wheat and rice genes

AS Type	Conserved Introns ^a	Conserved Events ^b
AD	2	0
AA	28	8
SE	0	0
RI	216	11
Total	232	19

^aConserved introns correspond to the number of introns that are conserved between wheat and rice and show the indicated AS type in wheat (not necessarily in rice). ^bConserved events correspond to the number of conserved introns with the same AS type in both wheat and rice.

transposons in the Triticeae Repeat Sequence Database and/or Genetic Information Research Institute repetitive databases, suggesting that 7% of exons might have originated by the recruitment of transposable elements (Supplemental Table S17).

Comparative analysis of gene exon-intron structure revealed that out of 1,975 wheat genes, 168 (8.5%) were subjected to loss of intronic sequences that were otherwise present in the orthologous genes of the model genomes. Sixteen out of 168 genes (10%) were from nonsyntenic regions. Among these genes, 105 (63%) contained PTCs and, therefore, were considered to be pseudogenes. The potential mechanism for the origin of these genes could be retroposition, during which a copy of a parental gene is reverse transcribed and inserted into a new genomic location (Wang et al., 2006; Kaessmann et al., 2009).

To determine the extent of structural divergence between homeologous copies of wheat genes, we compared a set of 86 and 20 gene pairs between chromosomes 3A and 3B and chromosomes 3A and 3D, respectively. In spite of the recent divergence between the wheat genomes (approximately 2.7 million years ago), these genes demonstrated a remarkable level of structural divergence (Fig. 2B). The proportion of lost and acquired exonic sequences between 3A and 3B (1.5 and three times higher, respectively) and 3A and 3D (6.5 and 5.3 times higher, respectively) was higher than that observed in the rice-*B. distachyon* comparison. The proportion of conserved exons between 3A and 3B and between 3A and 3D, respectively, was nearly two and 1.7 times higher than that between wheat and the model grass genomes.

Rates of Coding Sequence Evolution in Syntenic Regions of Grass Genomes

Redundancy created by polyploidy can change the dynamic of coding sequence evolution by relaxing selection and providing opportunities for the accumulation of new mutations that may impact gene function. Here, we used two complementary approaches to assess the rates of coding sequence evolution in the wheat genome. First, we assessed the d_N/d_S rates from pairwise comparisons of 1,022 orthologous sets of genes to identify genes showing evidence of directional selection ($d_N/d_S > 1$; Yang and Nielsen, 2000). The overall distribution of d_N/d_S values in the three possible pairwise comparisons among wheat, rice, and *B. distachyon* was

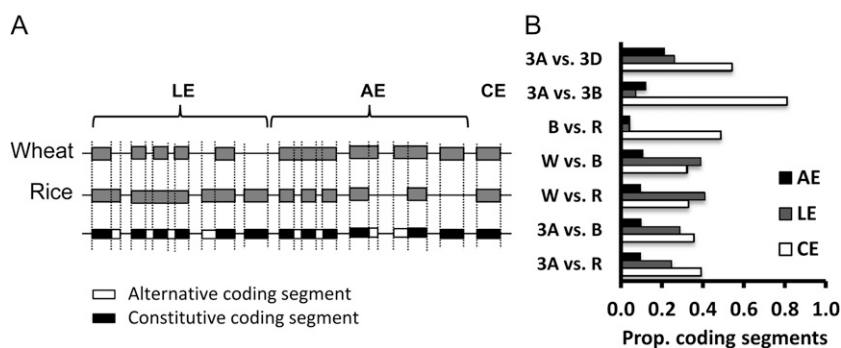


Figure 2. Proportion of alternative and conserved coding segments between wheat and the model genomes. A, Classification of coding segments used for comparison of gene exon-intron structure among wheat, rice, and *B. distachyon*. Only the wheat-rice comparison is shown. The protein isoforms of rice or *B. distachyon* were aligned to orthologous gene models in wheat. Differences in exon-intron structure in these pairwise comparisons were referred to as coding segments. Thus, each exon in our analysis was represented by a combination of several coding segments. Coding segments that were present in both compared orthologs were referred to as constitutive coding segments; coding segments that were present in only one of the two compared orthologs were referred to as alternative coding segments. The following categories of minievents resulting in gene structure changes were recorded: conserved exons (CE), acquired exons (AE), and lost exons (LE). Both AE and LE correspond to alternative coding segments; CE corresponds to a subset of constitutive coding segments. B, The proportion of AE, LE, and CE between the compared genes, relative to the total number of coding segments, was used to assess the level of gene structure conservation among orthologous genes of wheat (W), *B. distachyon* (B), and rice (R). Gene structure evolution was compared between wheat chromosome 3A and model genomes (3A versus R, 3A versus B), between two model grass genomes (B versus R), between a set of wheat genes located on other chromosomes (non-3A) and model genomes (W versus R, W versus B), and between homeologous genes on wheat chromosomes 3A, 3B, and 3D (3A versus 3B, 3A versus 3D).

similar and showed no statistically significant differences according to a nonparametric Wilcoxon rank-sum test (Fig. 3A). The estimates of d_N/d_S among pairwise comparisons were highly correlated (Spearman rank correlation = 0.82–0.91, $P < 2.2e^{-16}$), suggesting that the rates of mutations at synonymous and non-synonymous sites were gene specific (Fig. 3D). Only four genes in the wheat lineage (casein kinase I isoform δ -like, rhomboid family protein, tetratricopeptide repeat protein5-like, and ABC transporter C family) had $d_N/d_S > 1$ (Supplemental Table S18). BLASTN analysis (similarity, 80% or greater; alignment length, 100 bp or greater) did not detect duplicated copies of these genes on chromosome 3A. Analysis of protein sequences of these genes revealed an accumulation of lineage-specific amino acid changes in wheat, consistent with an increased d_N/d_S ratio. No PTCs were detected in the aligned portions of coding sequences.

To investigate the relationship between the chromosomal position of a gene and the rate of accumulation of nonsynonymous mutations, we analyzed the distribution of the d_N/d_S ratio along wheat chromosome 3A by plotting average d_N/d_S ratios calculated in a sliding window of five genes. High variation in d_N/d_S estimates was found along chromosome 3A, with only two chromosomal regions showing elevated d_N/d_S . One of these regions was located on the short arm and another one in the pericentromeric region of wheat chromosome 3A (Fig. 3D). Only one gene (tetratricopeptide repeat protein5-like) in the pericentromeric region had $d_N/d_S > 1$.

At the early stages of polyploid evolution, it is probable that many genes can become expressed pseudogenes whose function is impaired by an accumulation of PTCs. To test this possibility and estimate the frequency of nonfunctional expressed genes in the wheat genome, we identified orthologous open reading frames (ORFs) for 1,085 wheat transcripts by performing reciprocal BLASTN comparisons and selecting best hits (greater than 60% of cumulative identity percentage and greater than 70% cumulative alignment length percentage) in the syntenic regions of rice and *B. distachyon* genomes (for details, see Supplemental Material). Thirty-eight percent of these transcripts contained PTCs, suggesting that they are processed pseudogenes. No correlation was found between the occurrence of PTCs and upstream homopolymeric repeats (greater than 5 bp; Supplemental Material), suggesting that overcall/undercall errors prevalent in 454 data were not the major source of PTC origin. About 36% of genes on 3B and 3D homeologs have PTCs, which is similar to what we found on chromosome 3A.

The distribution of PTCs in orthologous sets of genes was compared with the distribution of exon loss/acquisition (LE/AE) events and d_N/d_S estimates. Structurally rearranged genes tended to have more PTCs (56 out of 162) than genes that have not undergone LE/AE (53 out of 860) in the wheat lineage (χ^2 test, $P < 0.001$). Most of the PTCs were due to frame-shift mutations. After correcting for frame shift, only 11% of genes still showed PTCs, which is comparable to 9.7%, the proportion of PTCs in genes that showed no exon gain or

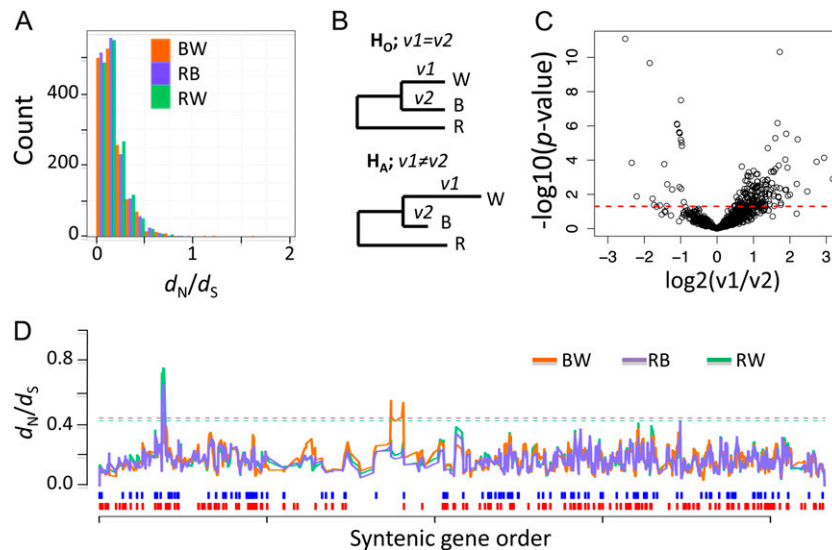


Figure 3. Evolution of coding sequences in the wheat genome. A, Distribution of pairwise estimates of d_N/d_S in a set of orthologous genes from wheat (W), *B. distachyon* (B), and rice (R). B, H_0 and H_A are null (codon mutation rates in the wheat and *B. distachyon* lineages are equal; $v_1 = v_2$) and alternative (codon mutation rates in the wheat and *B. distachyon* lineages are different; $v_1 \neq v_2$) hypotheses, respectively; v_1 and v_2 are expected codon mutation rates in wheat and *B. distachyon*, respectively. C, \log_2 ratio of codon mutation rates in the wheat (v_1) and *B. distachyon* (v_2) lineages estimated for an orthologous set of 986 genes (Supplemental Table S19). The significance threshold ($P \leq 0.05$) is shown by the red dashed line. D, Distribution of d_N/d_S estimates, PTCs (blue bars), and LE/AE events (red bars) along wheat chromosome 3A. The 95th percentile of d_N/d_S ratio distribution in a window of five genes (dashed lines) was calculated by permutation (see “Materials and Methods”).

loss. No significant differences in pairwise d_N/d_S estimates were found between gene sets grouped according to the presence/absence of PTCs (Wilcoxon rank sum test, $P > 0.1$) or LE/AE events (Wilcoxon rank sum test, $P > 0.05$). The majority of structurally evolved genes did not show evidence for relaxation of selection; d_N/d_S estimates of only 3.8% of these genes were higher than 0.5.

To gain better insights into the evolutionary dynamics of coding sequences in the wheat genome, we compared the rates of codon evolution along the wheat and *B. distachyon* lineages using rice as an outgroup (Fig. 3, B and C). The codon evolution models allow for explicit modeling of the evolution of a protein sequence by considering codons as units of evolution while taking into account changes in synonymous and nonsynonymous sites (Muse and Gaut, 1994) rather than separately estimating substitution rates at the single nucleotide level (Fig. 3B). The relative rate test included a set of 986 orthologous triplets of genes from *B. distachyon*, rice, and wheat. Among these sets, 191 showed statistically significant differences ($P \leq 0.05$) in the rate of codon evolution (Supplemental Table S19), out of which 167 (87%) showed increased codon mutation rates in the wheat lineage compared with that in *B. distachyon* [$\log_2(v1/v2) > 0$; Fig. 3C]. This estimate, even taking into account the 1.9% probability of including nonorthologous genes into the analysis due to contamination, is still substantial. On average, the codon mutation rate was 1.4 times higher in wheat than in *B. distachyon*. The Gene Ontology annotation of genes with elevated rates of nonsynonymous substitutions showed that the majority did not have a specific function assigned in the Gene Ontology database. Those that could be classified (48 genes) belonged to various biological processes. Interestingly, out of the 15 genes that could be classified into Gene Ontology categories according to their biological functions, six were protein kinase members.

DISCUSSION

We analyzed evolutionary processes that can impact the coding potential of the recently originated polyploid wheat genome through modifications of gene structure, coding sequence, and AS. More than 370 Mb of wheat genomic sequence was analyzed to predict genes by aligning homeolog-specific transcript assemblies. More than 6,600 complete and partial gene structures were predicted in chromosome 3A contig assemblies. Comparative genomics was used to establish syntenic relationships between wheat chromosome 3A and model grass genomes and to build a framework for the evolutionary analysis of coding regions. Even though a detectable level of contamination from other wheat chromosomes was found in the flow-sorted 3A material (up to 13%) and errors for separating homeologous transcripts (5.7%) can introduce some bias in our evolutionary rate estimates, our results suggest that coding regions of the wheat genome have undergone

complex historical changes and that the size of the wheat genome and polyploidy are important factors to consider for understanding its dynamic evolution.

Expansion of genome size in the Triticeae lineage associated with the proliferation of repetitive elements has impacted not only the large-scale structural organization of the wheat genome (Gu et al., 2006; Choulet et al., 2010; Massa et al., 2011) but possibly has had a significant impact on gene structure evolution. A high frequency of long terminal repeat transposons in the wheat genome showing evidence of recent activity (Charles et al., 2008; Choulet et al., 2010) may have substantially accelerated the rate of retrogene origin. Our results are consistent with this possibility and are also supported by the earlier discovery of new genes in the wheat genome whose origin could be linked with transposon activity (Akhunov et al., 2007; Choulet et al., 2010; Wicker et al., 2010). Other studies also demonstrated that transposon activity could result in the origin of new genes (Lal et al., 2003; Wang et al., 2006; Zhu et al., 2009).

The high frequency of gene structural rearrangements in the wheat genome can be explained by the interplay of two other factors: the relaxation of selection resulting from WGD, and selection on dosage-sensitive regulatory pathways or gene complexes. According to the “gene balance model” (Birchler and Veitia, 2007; Freeling, 2009), dosage-insensitive genes have a tendency to deteriorate over time through the accumulation of deleterious mutations, whereas dosage-sensitive genes are subjected to purifying selection and tend to be retained. These predictions are consistent with findings that genes showing a higher connectivity level in networks (Severin et al., 2011), or contributing more to gene expression (Schnable et al., 2011), tend to be retained in ancient polyploids. In our study, selection against gene structure modifications was evident in the diploid model genomes, which showed a reduced number of LE/AE events compared with the wheat genome. This suggests that polyploidy can contribute to the increased accumulation of nonfunctional structural variants of genes. Similarly, our finding that 38% of expressed genes in the wheat genome contain PTCs supports the relaxation of selection hypothesis. The high incidence of PTCs among structurally rearranged genes and retrogenes, as well as the preferential loss of exonic sequences, are indicative of the relaxation of selection and ongoing degeneration of duplicated genes in the wheat genome. This is in contrast to the finding that only 27% of retrogenes in the diploid rice genome are processed pseudogenes (Wang et al., 2006). It is possible that during early stages of polyploid evolution, the accumulation of new structural variants occurs almost neutrally. At the later stages of evolution, when most of the genome becomes diploidized, functional constraints on structural variants of genes increase, resulting in the preferential retention of functionally active genes.

Relaxation of selection in the wheat genome is consistent with results from the relative rate test, which showed

an accelerated accumulation of nonsynonymous mutations in the wheat lineage. An accelerated rate of codon evolution was observed for 19% of genes in either the wheat or *B. distachyon* lineage, suggesting significant levels of heterogeneity in the rates of gene evolution across the syntenic regions of grass genomes. No obvious effects of wheat chromosomal position or gene function were observed upon rates of codon evolution. According to the results of d_N/d_S estimates, which showed a strong correlation among the three possible pairwise genome comparisons, variation in the rates of nonsynonymous mutations seems to be defined by gene-specific functional attributes. The differences in codon mutation rates along the *B. distachyon* lineage also suggest that genes in diploid genomes are under stronger selective constraint than those in polyploid genomes. Certainly, we cannot exclude the possibility that some of the differences in codon mutation rates between the *B. distachyon* and wheat lineages were caused by an accelerated rate of mutation in the wild diploid ancestors of wheat. However, our previous analysis of mutation rates in diploid and polyploid wheat suggests that the majority of nonsynonymous mutations are associated with polyploid wheat evolution (Akhunov et al., 2008).

Estimates of AS obtained for each wheat subgenome using homeolog-specific alignments were within the range (25%–42%) previously predicted for the rice, Arabidopsis, and *B. distachyon* genomes (Campbell et al., 2006; Wang and Brendel, 2006; Filichkin et al., 2010). Consistent with previous studies, the dominant type of AS event in wheat was intron retention, followed by alternative donor and acceptor splicing events (Campbell et al., 2006; Wang and Brendel, 2006; Barbazuk et al., 2008). Similar to other plant systems, exon skipping represented only a small (4%–6%) fraction of AS events (Wang and Brendel, 2006), and intron retention mostly (91%) resulted in premature stop codons (Filichkin et al., 2010). It is suggested that the majority of transcripts resulting from this type of AS are targeted by the nonsense-mediated decay and regulated unproductive splicing and translation pathways, which play an important role in the regulation of functional transcript levels (Lewis et al., 2003; Maquat, 2004).

Comparative analysis of AS patterns between the wheat genomes revealed a significant number of new transcript isoforms in duplicated genes acquired since divergence from a common ancestor. Previous studies demonstrated the interdependence of gene duplication and AS (Roux and Robinson-Rechavi, 2011) and suggested that neutral processes associated with the relaxation of selection can drive the accumulation of new splice isoforms in duplicated genes (Lev-Maor et al., 2007). Fast changes in RI splice variants previously reported for polyploid *Brassica* spp. (Zhou et al., 2011) suggest that WGD may have a substantial impact on the divergence of AS patterns between the homeologs. It is possible that WGDs in wheat have contributed to transcriptome diversity not only by combining transcriptomes of diverged diploid ancestors but also by

relaxing functional constraints on AS. Thus, even though we do not see significant differences in the level of AS in each individual wheat homeolog, the divergence of AS between duplicated genes (42%–61%) can increase the overall transcript isoform diversity in the polyploid genomes.

By analyzing AS conservation using the approach developed by Wang and Brendel (2006), we obtained results that were similar to those observed in a rice-Arabidopsis comparison, where only 8% to 9% of conserved introns had the same type of AS events in both wheat and rice. In spite of a higher divergence time between rice and Arabidopsis (130 million years ago) than between rice and wheat (40 million years ago), we observed a similar level of AS conservation. This could be a consequence of the approach used to predict the conserved AS events; by selecting conserved introns, we may have enriched our sample for genes with AS events that are using evolutionarily conserved mechanisms of gene expression regulation (Lewis et al., 2003; Maquat, 2004). Another possibility is that the majority of AS events in plants are selectively neutral and their fate is defined by stochastic evolutionary processes, while only 8% to 9% of AS events are involved in biologically important functions and, therefore, are widely conserved throughout diverged plant lineages. Alternatively, the rate of gene space evolution in the wheat genome may be accelerated due to polyploidy or high repetitive DNA content, which, in turn, can result in a faster rate of AS evolution.

CONCLUSION

In conclusion, it seems that neutral processes largely define the evolution of the wheat genome coding regions. It is likely that genetic redundancy created by WGDs allows for an accelerated accumulation of AS isoforms, nonsynonymous and PTC mutations, and gene structure rearrangements leading to the degeneration of duplicated gene complements. Even though these processes mostly contribute to genome diploidization, they have potential to accelerate the origin of new functional variation, providing raw material for selection. Therefore, it is plausible that a high level of polyploid genome plasticity may have played an important role in broadening both genetic and phenotypic diversity in wheat. It will be of great interest to investigate the contribution of the molecular processes described in our study to the origin of new variants of genes and to assess their importance in phenotypic evolution in the context of crop domestication and improvement.

MATERIALS AND METHODS

Sequencing of Flow-Sorted Chromosomal DNA and Assembly

The chromosome 3A double ditelosomic lines in the genetic background of wheat (*Triticum aestivum* 'Chinese Spring') were used to isolate chromosome arm 3AS- and 3AL-specific DNA by flow sorting (Kubaláková et al., 2002; Doležel

et al., 2007). In addition to flow-sorted chromosomal DNA, single-read sequencing was performed for a set of 2,743 BAC clones distributed among 1,104 BAC contigs assembled using the high information content fingerprint data obtained for 190,464 BAC clones from wheat chromosome 3A (http://wggrc.plantpath.ksu.edu/wheat/3A/3A_index.html). All genomic libraries were sequenced using 454 Titanium chemistry in the Kansas State University Integrated Genomics Facility (www.ksre.ksu.edu/igenomics). The combined data set generated for the flow-sorted chromosome arms and BAC clones corresponded to 9.3× coverage of wheat chromosome 3A (Supplemental Table S1; NCBI accession no. SRA045666). More detailed description of a sequencing protocol and assembly parameters can be found in the Supplemental Material.

Predicting Exon-Intron Structure

The evidence-based prediction of exon-intron structure in wheat contigs was performed using wheat transcriptome sequence data, which comprised 454 sequence data (<http://wheatgenomics.plantpath.ksu.edu/snp/>; SRA048705), full-length cDNA sequences (<http://trifldb.psc.riken.jp/index.pl>), and wheat ESTs from the NCBI database.

The 454 transcriptome data generated for eight wheat cultivars, consisting of about 5.8 million reads, was assembled using MIRA software (version 3.03). This program uses an iterative sequence assembly approach that can refine contig assemblies after each iteration step by putting reads that contain mutations consistently differentiating them from the rest of the reads in a contig into separate contigs (Chevreux et al., 2004). These settings are optimized for the assembly of ESTs ("est" option of the MIRA assembler) and the separation of transcript isoforms originating from different copies of homeologous or paralogous genes in the wheat genome (Chevreux et al., 2004; Supplemental Table S12). Since the average divergence of genes duplicated during wheat polyploidization is about 2% to 4% in coding regions (Dvorak et al., 2006), we would expect to have about 10 to 16 single-base substitutions per 500-bp read that differentiate one wheat subgenome from another.

In order to infer the exon-intron structure of genes in the polyploid wheat genome, we preselected homeolog-specific transcript assemblies, full-length cDNA, and ESTs by aligning them against wheat contigs using BLAT (Kent, 2002). Transcripts showing sequence similarity greater than 98.5% and minimum alignment length greater than 200 bp were used for further analysis. These thresholds were chosen to preclude the misalignment of duplicated genes to the wrong homeologous copy of a gene in the wheat genome. The accuracy of genome assignment was based on counting the proportion of mutations that differentiate 86 homeologous gene pairs identified in wheat chromosomes 3A and 3B (see "Results") and that are also found to correctly match the respective genome in transcript/genomic sequence alignments. The results of this analysis suggest that 92% of homeologous mutations can be correctly assigned to a genome. Spliced alignments for gene prediction were created using the GMAP program integrated into the PASA gene prediction pipeline (<http://pasa.sourceforge.net>; Supplemental Table S20).

AS

Gene annotations produced by aligning homeolog-specific transcript assemblies against wheat genomic sequences were extracted from the PASA database for estimating AS. Characterization of AS was performed separately in three sets of genomic sequence data: contigs/scaffolds generated for chromosome 3A in our study, contigs of chromosome 3B BAC clones generated by Choulet et al. (2010), and contigs of BAC clones distributed across the wheat genome (NCBI database; Supplemental Table S11).

AS was compared between homeologous copies of genes on wheat chromosomes 3A and 3B by counting the number of shared and different AS events, including skipped exons, retained introns, and alternative donor and acceptor variants.

The second method for comparing AS is based on the approach suggested by Wang and Brendel (2006). Briefly, conserved introns in orthologous sets of genes between rice (*Oryza sativa*) and wheat were identified by matching all rice introns and flanking 30-bp exons against wheat introns and flanking exons with TBLASTX (E value < e^{-4}), and only those hits that contained at least 10 bp from both flanking exons were selected.

Rates of Molecular Evolution

The ORFs of orthologous sets of genes from rice, *Brachypodium distachyon*, and wheat were aligned using the MUSCLE program (version 3.8.31; [www](http://www.drive5.com/muscle/).

www.drive5.com/muscle/) to estimate rates of molecular evolution in coding sequences. Aligned ORFs were filtered to remove those that (1) were shorter than 300 bp, (2) included gaps longer than 100 bp, or (3) included gaps covering more than 10% of alignment length. The rates of evolution were contrasted between the wheat and *B. distachyon* lineages using rice as an outgroup. Both the *B. distachyon* and wheat lineages diverged from rice about 50 million years ago (Paterson et al., 2004). Two tests were applied to assess the rate of codon evolution in the alignments. The first test was performed using the yn00 program from the PAML package (version 4.4d; Yang, 2007) with default parameters (icode = 0, weighting = 0, commonf3x4 = 0). The program was used to estimate d_N/d_S ratios in wheat-rice and *B. distachyon*-rice pairwise comparisons using the method of Yang and Nielsen (2000).

The relative rate test implemented in the HyPhy program (version 2.0020110606beta; www.hyphy.org; Pond et al., 2005) was applied to compare the rates of codon evolution in the *B. distachyon* and wheat lineages using rice as an outgroup and the following options: data type, codon; genetic code, universal; outgroup, rice; standard model, GY94; model options, global. In this test, the codon evolution model was used for modeling nucleotide substitution rates (Goldman and Yang, 1994; Muse and Gaut, 1994). The model specifically focuses on estimating two separate parameters for synonymous (α) and nonsynonymous (β) substitution rates. The relative rate test allows for the detection of significant changes in the relative rates of α and β by comparing the two alternative codon evolution models using the likelihood ratio test: model H_0 assumes that the rates of codon evolution along the wheat ($v1$) and *B. distachyon* ($v2$) lineages are equal ($v1 = v2$), and model H_1 assumes that the rates of codon evolution along the wheat and *B. distachyon* lineages are different ($v1 \neq v2$). A more detailed description of the relative rate test using the codon evolution model can be found in Muse and Gaut (1994).

Evolution of Gene Structure

For this analysis, the alternative protein isoforms of *B. distachyon* and rice were splice aligned against the genomic sequence of wheat, and the protein isoforms of rice were aligned against the genomic sequence of *B. distachyon*. Only those alignments that contained at least two exons were considered. We used the average proportion of acquired, lost, and conserved exonic segments relative to the total number of coding segments among all possible pairwise comparisons between orthologs (Fig. 2A) as a measure of similarity between gene structures of the compared genomes.

First, we compared the exon-intron structures of orthologous genes between wheat and the two grass genomes, rice and *B. distachyon*. Three types of evolutionary events resulting in exon-intron structural changes were recorded: (1) loss of exonic segments; (2) acquisition of exonic segments; and (3) conservation of exonic segments (Fig. 3A). For this purpose, the protein isoforms predicted in the model grass genomes were splice aligned with the wheat contigs/scaffolds. The inferred exon-intron structure was compared with that predicted by aligning wheat ESTs/cDNAs. Annotations of exon-intron structure and corresponding coding sequences for the rice and *B. distachyon* genomes were downloaded from public databases (www.brachypodium.org/ and rice.plantbiology.msu.edu). The translated sequences of all mRNA isoforms from syntenic regions of *B. distachyon* and rice genomes were splice aligned against wheat genomic sequences using the GeneWise program (www.ebi.ac.uk/Tools/Wise2) with optimized settings (-splice flat; -null flat; -alg 2193; -both strands). The quality score of spliced alignments generated by GeneWise was kept above 35, as recommended by the software developer. The structures of orthologous genes in rice, *B. distachyon*, and wheat were pairwise compared. Differences in exon-intron structure were referred to as "coding segments." Thus, each exon in our analysis was represented by a combination of several coding segments. Coding segments that were present in both compared species were referred to as constitutive coding segments, and coding segments that were present in only one of the two compared species were referred to as alternative coding segments. The proportion of alternative and constitutive coding segments between compared genes, relative to the total number of coding segments, was calculated for each orthologous gene set. The proportion of alternative coding segments per gene was averaged across all orthologous gene sets and used as the estimate of gene structure conservation between the compared genomes. The description of evolutionary changes in exon-intron structure used in this analysis is presented in Figure 2A.

Changes in gene structure were further characterized to understand the molecular mechanisms involved in their origin. The sequences of newly acquired exonic fragments in the wheat lineage were compared against the databases of repetitive elements (Genetic Information Research Institute and

Triticeae Repeat Sequence Database) and proteins (NCBI) using BLAST. For the identification of retroposition events resulting from the insertion of reverse-transcribed mRNA, the structures of genes in the wheat genome were compared with that of the model genomes.

The distribution of the d_N/d_S ratio, premature termination codons, and LE/AE events in the wheat lineage were plotted along chromosome 3A according to the syntenic gene order. The d_N/d_S was calculated in a sliding window of five genes for each pairwise comparison between wheat, rice, and *B. distachyon*. The d_N/d_S ratio threshold for a window of five genes corresponds to the 95th percentile of the mean d_N/d_S ratio estimated for 100,000 sets of five genes, sampled randomly with replacement from the entire data set.

Sequence data from this article can be found in the NCBI data libraries under accession numbers SRA012746, SRA045666, SRA048705, and PRJNA80879. Accession numbers of BAC clone sequences are JQ354542 to JQ354560. The contig assemblies and alignments of orthologous genes are also available for download from http://129.130.90.211/chr3A_data. Wheat transcriptome assemblies can be searched using BLAST at the wheat SNP project Web site (<http://wheatgenomics.plantpath.ksu.edu/snp/>).

Supplemental Data

The following materials are available in the online version of this article.

Supplemental Figure S1. Relationship between chromosome 3A contig length and read coverage.

Supplemental Figure S2. Distribution of the number of alignment positions at each coverage depth (including the gaps at all positions) for chromosome 3A assemblies.

Supplemental Figure S3. Coverage of the wheat chromosome 3A gene space.

Supplemental Figure S4. Comparison of wheat chromosome 3A with the *B. distachyon* genome.

Supplemental Figure S5. Comparison of wheat chromosome 3A with the sorghum genome.

Supplemental Figure S6. Comparison of wheat chromosome 3A with the rice genome.

Supplemental Figure S7. Comparison of gene order between a SNP map of chromosome 3D and the SGO map of chromosome 3A.

Supplemental Figure S8. Intragenomic duplications in wheat.

Supplemental Figure S9. Examples of AS types.

Supplemental Figure S10. Functional classification of genes on the 3A SGO map.

Supplemental Figure S11. Distribution of sequence similarity levels in the coding regions of the wheat genome.

Supplemental Table S1. Summary of sequence data used in the assembly of wheat chromosome 3A.

Supplemental Table S2. Purity assessment of amplified flow-sorted arms of wheat chromosome 3A.

Supplemental Table S3. Comparison of chromosome 3A BAC clone sequences with 454 contigs and scaffolds.

Supplemental Table S4. Classes of repetitive elements masked in contig assemblies.

Supplemental Table S5. Comparison of chromosome 3A contigs with coding sequences of model genomes (rice, sorghum, and *B. distachyon*).

Supplemental Table S6. Comparison of the repeat-masked chromosome 3A contigs and scaffolds with the rice, *B. distachyon*, and sorghum genomes.

Supplemental Table S7. Distribution of BLASTN hits between wheat chromosome 3A genes and three cereal genomes (rice, *B. distachyon*, and sorghum).

Supplemental Table S8. Chromosome 3A contigs and scaffolds ordered using syntenic relationships between wheat and sequenced model grass genomes (SGO).

Supplemental Table S9. Interchromosomal duplications in the wheat genome.

Supplemental Table S10. Identification of chromosome 3A centromere boundaries.

Supplemental Table S11. BAC contig sequences downloaded from the NCBI database.

Supplemental Table S12. The 454 transcriptome data generated for eight wheat cultivars.

Supplemental Table S13. Counts of AS events in a set of homeologous genes identified between wheat chromosomes 3A and 3B.

Supplemental Table S14. Proportion of alternative and conserved coding segments between wheat and the model genomes.

Supplemental Table S15. Genes with acquired exonic sequences specific to the wheat lineage.

Supplemental Table S16. Validation of acquired exonic sequences by reverse transcription-PCR.

Supplemental Table S17. Characterization of acquired exonic sequences.

Supplemental Table S18. d_N/d_S ratio estimates for wheat-rice, wheat-*B. distachyon*, and rice-*B. distachyon* pairwise comparisons.

Supplemental Table S19. Comparison of the rates of codon evolution in the *B. distachyon* and wheat lineages using rice as an outgroup.

Supplemental Table S20. Prediction of exon-intron structure performed using the GMAP program integrated into the PASA gene prediction pipeline.

Supplemental Materials and Methods S1.

Received August 7, 2012; accepted October 29, 2012; published November 1, 2012.

LITERATURE CITED

- Akhunov ED, Akhunova AR, Anderson OD, Anderson JA, Blake N, Clegg MT, Coleman-Derr D, Conley EJ, Crossman CC, Deal KR, et al (2008) Purifying selection and gene conversion in polyploid wheat evolution. *In* Proceedings of the 11th International Wheat Genetics Symposium. Sydney University Press, Sydney, Australia, pp 1–3
- Akhunov ED, Akhunova AR, Anderson OD, Anderson JA, Blake N, Clegg MT, Coleman-Derr D, Conley EJ, Crossman CC, Deal KR, et al (2010) Nucleotide diversity maps reveal variation in diversity among wheat genomes and chromosomes. *BMC Genomics* **11**: 702
- Akhunov ED, Akhunova AR, Dvorak J (2007) Mechanisms and rates of birth and death of dispersed duplicated genes during the evolution of a multigene family in diploid and tetraploid wheats. *Mol Biol Evol* **24**: 539–550
- Akhunov ED, Akhunova AR, Linkiewicz AM, Dubcovsky J, Hummel D, Lazo G, Chao S, Anderson OD, David J, Qi L, et al (2003) Synteny perturbations between wheat homoeologous chromosomes caused by locus duplications and deletions correlate with recombination rates. *Proc Natl Acad Sci USA* **100**: 10836–10841
- Akhunova AR, Matniyazov RT, Liang H, Akhunov ED (2010) Homoeolog-specific transcriptional bias in allopolyploid wheat. *BMC Genomics* **11**: 505
- Ast G (2004) How did alternative splicing evolve? *Nat Rev Genet* **5**: 773–782
- Båga M, Glaze S, Mallard CS, Chibbar RN (1999) A starch-branching enzyme gene in wheat produces alternatively spliced transcripts. *Plant Mol Biol* **40**: 1019–1030
- Barbazuk WB, Fu Y, McGinnis KM (2008) Genome-wide analyses of alternative splicing in plants: opportunities and challenges. *Genome Res* **18**: 1381–1392
- Bartoš J, Vlček C, Choulet F, Džunková M, Cvíková K, Safář J, Simková H, Pačes J, Strnad H, Sourdille P, et al (2012) Intraspecific sequence comparisons reveal similar rates of non-collinear gene insertion in the B and D genomes of bread wheat. *BMC Plant Biol* **12**: 155
- Birchler JA, Veitia RA (2007) The gene balance hypothesis: from classical genetics to modern genomics. *Plant Cell* **19**: 395–402

- Bottley A, Koebner RM** (2008) Variation for homoeologous gene silencing in hexaploid wheat. *Plant J* **56**: 297–302
- Campbell MA, Haas BJ, Hamilton JP, Mount SM, Buell CR** (2006) Comprehensive analysis of alternative splicing in rice and comparative analyses with Arabidopsis. *BMC Genomics* **7**: 327
- Chalupska D, Lee HY, Faris JD, Evrard A, Chalhoub B, Haselkorn R, Gornicki P** (2008) Acc homoeoloci and the evolution of wheat genomes. *Proc Natl Acad Sci USA* **105**: 9691–9696
- Charles M, Belcram H, Just J, Huneau C, Viollet A, Couloux A, Segurens B, Carter M, Huteau V, Coriton O, et al** (2008) Dynamics and differential proliferation of transposable elements during the evolution of the B and A genomes of wheat. *Genetics* **180**: 1071–1086
- Chen M, Ha M, Lackey E, Wang J, Chen ZJ** (2008) RNAi of met1 reduces DNA methylation and induces genome-specific changes in gene expression and centromeric small RNA accumulation in Arabidopsis allopolyploids. *Genetics* **178**: 1845–1858
- Chen ZJ** (2007) Genetic and epigenetic mechanisms for gene expression and phenotypic variation in plant polyploids. *Annu Rev Plant Biol* **58**: 377–406
- Chevreux B, Pfisterer T, Drescher B, Driesel AJ, Müller WE, Wetter T, Suhai S** (2004) Using the miraEST assembler for reliable and automated mRNA transcript assembly and SNP detection in sequenced ESTs. *Genome Res* **14**: 1147–1159
- Choulet F, Wicker T, Rustenholz C, Paux E, Salse J, Leroy P, Schlub S, Le Paslier MC, Magdelenat G, Gonthier C, et al** (2010) Megabase level sequencing reveals contrasted organization and evolution patterns of the wheat gene and transposable element spaces. *Plant Cell* **22**: 1686–1701
- Comai L** (2005) The advantages and disadvantages of being polyploid. *Nat Rev Genet* **6**: 836–846
- Devos KM** (2010) Grass genome organization and evolution. *Curr Opin Plant Biol* **13**: 139–145
- Doležel J, Kubaláková M, Paux E, Bartos J, Feuillet C** (2007) Chromosome-based genomics in the cereals. *Chromosome Res* **15**: 51–66
- Dvorak J, Akhunov ED** (2005) Tempos of gene locus deletions and duplications and their relationship to recombination rate during diploid and polyploid evolution in the Aegilops-Triticum alliance. *Genetics* **171**: 323–332
- Dvorak J, Akhunov ED, Akhunov AR, Deal KR, Luo MC** (2006) Molecular characterization of a diagnostic DNA marker for domesticated tetraploid wheat provides evidence for gene flow from wild tetraploid wheat to hexaploid wheat. *Mol Biol Evol* **23**: 1386–1396
- Dvorák J, Terlizzi P, Zhang HB, Resta P** (1993) The evolution of polyploid wheats: identification of the A genome donor species. *Genome* **36**: 21–31
- Dvorák J, Zhang HB** (1990) Variation in repeated nucleotide sequences sheds light on the phylogeny of the wheat B and G genomes. *Proc Natl Acad Sci USA* **87**: 9640–9644
- Fan C, Zhang Y, Yu Y, Rounsley S, Long M, Wing RA** (2008) The subtelomere of *Oryza sativa* chromosome 3 short arm as a hot bed of new gene origination in rice. *Mol Plant* **1**: 839–850
- Fawcett JA, Rouzé P, Van de Peer Y** (2012) Higher intron loss rate in Arabidopsis thaliana than A. lyrata is consistent with stronger selection for a smaller genome. *Mol Biol Evol* **29**: 849–859
- Filichkin SA, Priest HD, Givan SA, Shen R, Bryant DW, Fox SE, Wong WK, Mockler TC** (2010) Genome-wide mapping of alternative splicing in Arabidopsis thaliana. *Genome Res* **20**: 45–58
- Force A, Lynch M, Pickett FB, Amores A, Yan YL, Postlethwait J** (1999) Preservation of duplicate genes by complementary, degenerative mutations. *Genetics* **151**: 1531–1545
- Freeling M** (2009) Bias in plant gene content following different sorts of duplication: tandem, whole-genome, segmental, or by transposition. *Annu Rev Plant Biol* **60**: 433–453
- Gaeta RT, Yoo SY, Pires JC, Doerge RW, Chen ZJ, Osborn TC** (2009) Analysis of gene expression in resynthesized Brassica napus allopolyploids using Arabidopsis 70mer oligo microarrays. *PLoS ONE* **4**: e4760
- Goldman N, Yang Z** (1994) A codon-based model of nucleotide substitution for protein-coding DNA sequences. *Mol Biol Evol* **11**: 725–736
- Gu YQ, Coleman-Derr D, Kong X, Anderson OD** (2004) Rapid genome evolution revealed by comparative sequence analysis of orthologous regions from four Triticeae genomes. *Plant Physiol* **135**: 459–470
- Gu YQ, Salse J, Coleman-Derr D, Dupin A, Crossman C, Lazo GR, Huo N, Belcram H, Ravel C, Charmet G, et al** (2006) Types and rates of sequence evolution at the high-molecular-weight glutenin locus in hexaploid wheat and its ancestral genomes. *Genetics* **174**: 1493–1504
- Han MV, Demuth JP, McGrath CL, Casola C, Hahn MW** (2009) Adaptive evolution of young gene duplicates in mammals. *Genome Res* **19**: 859–867
- Huang S, Sirikhachornkit A, Faris JD, Su X, Gill BS, Haselkorn R, Gornicki P** (2002) Phylogenetic analysis of the acetyl-CoA carboxylase and 3-phosphoglycerate kinase loci in wheat and other grasses. *Plant Mol Biol* **48**: 805–820
- Hughes AL** (1994) The evolution of functionally novel proteins after gene duplication. *Proc Biol Sci* **256**: 119–124
- International Brachypodium Initiative** (2010) Genome sequencing and analysis of the model grass Brachypodium distachyon. *Nature* **463**: 763–768
- International Rice Genome Sequencing Project** (2005) The map-based sequence of the rice genome. *Nature* **436**: 793–800
- Kaessmann H, Vinckenbosch N, Long M** (2009) RNA-based gene duplication: mechanistic and evolutionary insights. *Nat Rev Genet* **10**: 19–31
- Kashkush K, Feldman M, Levy AA** (2002) Gene loss, silencing and activation in a newly synthesized wheat allotetraploid. *Genetics* **160**: 1651–1659
- Kashkush K, Feldman M, Levy AA** (2003) Transcriptional activation of retrotransposons alters the expression of adjacent genes in wheat. *Nat Genet* **33**: 102–106
- Kent WJ** (2002) BLAT: the BLAST-like alignment tool. *Genome Res* **12**: 656–664
- Kihara H** (1944) Discovery of the DD-analyser, one of the ancestors of Triticum vulgare. (Japanese). *Agric Hortic* **19**: 889–890
- Koonin EV, Wolf YI** (2010) Constraints and plasticity in genome and molecular-phenome evolution. *Nat Rev Genet* **11**: 487–498
- Kubaláková M, Vrána J, Cíhalíková J, Simková H, Doležel J** (2002) Flow karyotyping and chromosome sorting in bread wheat (*Triticum aestivum* L.). *Theor Appl Genet* **104**: 1362–1372
- Lal SK, Giroux MJ, Brendel V, Vallejos CE, Hannah LC** (2003) The maize genome contains a helitron insertion. *Plant Cell* **15**: 381–391
- Lev-Maor G, Goren A, Sela N, Kim E, Keren H, Doron-Faigenboim A, Leibman-Barak S, Pupko T, Ast G** (2007) The “alternative” choice of constitutive exons throughout evolution. *PLoS Genet* **3**: e203
- Lewis BP, Green RE, Brenner SE** (2003) Evidence for the widespread coupling of alternative splicing and nonsense-mediated mRNA decay in humans. *Proc Natl Acad Sci USA* **100**: 189–192
- Lin JY, Stupar RM, Hans C, Hyten DL, Jackson SA** (2010) Structural and functional divergence of a 1-Mb duplicated region in the soybean (*Glycine max*) genome and comparison to an orthologous region from *Phaseolus vulgaris*. *Plant Cell* **22**: 2545–2561
- Long M, Betrán E, Thornton K, Wang W** (2003) The origin of new genes: glimpses from the young and old. *Nat Rev Genet* **4**: 865–875
- Lu T, Lu G, Fan D, Zhu C, Li W, Zhao Q, Feng Q, Zhao Y, Guo Y, Li W, et al** (2010) Function annotation of the rice transcriptome at single-nucleotide resolution by RNA-seq. *Genome Res* **20**: 1238–1249
- Luo MC, Deal KR, Akhunov ED, Akhunova AR, Anderson OD, Anderson JA, Blake N, Clegg MT, Coleman-Derr D, Conley EJ, et al** (2009) Genome comparisons reveal a dominant mechanism of chromosome number reduction in grasses and accelerated genome evolution in Triticeae. *Proc Natl Acad Sci USA* **106**: 15780–15785
- Lynch M, Conery JS** (2000) The evolutionary fate and consequences of duplicate genes. *Science* **290**: 1151–1155
- Maquat LE** (2004) Nonsense-mediated mRNA decay: splicing, translation and mRNP dynamics. *Nat Rev Mol Cell Biol* **5**: 89–99
- Marquez Y, Brown JW, Simpson C, Barta A, Kalyna M** (2012) Transcriptome survey reveals increased complexity of the alternative splicing landscape in Arabidopsis. *Genome Res* **22**: 1184–1195
- Massa AN, Wanjugi H, Deal KR, O'Brien K, You FM, Maiti R, Chan AP, Gu YQ, Luo MC, Anderson OD, et al** (2011) Gene space dynamics during the evolution of Aegilops tauschii, Brachypodium distachyon, Oryza sativa, and Sorghum bicolor genomes. *Mol Biol Evol* **28**: 2537–2547
- Mayer KFX, Martis M, Hedley PE, Simková H, Liu H, Morris JA, Steuernagel B, Taudien S, Roessner S, Gundlach H, et al** (2011) Unlocking the barley genome by chromosomal and comparative genomics. *Plant Cell* **23**: 1249–1263
- McFadden ES, Sears ER** (1944) The artificial synthesis of Triticum spelta. *Rec Soc Genet Am* **13**: 26–27
- McFadden ES, Sears ER** (1946) The origin of Triticum spelta and its free-threshing hexaploid relatives. *J Hered* **37**: 81–89, 107
- Muse SV, Gaut BS** (1994) A likelihood approach for comparing synonymous and nonsynonymous nucleotide substitution rates, with application to the chloroplast genome. *Mol Biol Evol* **11**: 715–724

- Nesbitt M, Samuel D (1996) From staple crop to extinction? The archaeology and history of the hulled wheats. In S Padulosi, K Hammer, J Heller, eds, *Hulled Wheats*, Vol 4. International Plant Genetic Resources Institute, Rome, pp 41–100
- Ni Z, Kim ED, Ha M, Lackey E, Liu J, Zhang Y, Sun Q, Chen ZJ (2009) Altered circadian rhythms regulate growth vigour in hybrids and allopolyploids. *Nature* **457**: 327–331
- Nomura T, Ishihara A, Yanagita RC, Endo TR, Iwamura H (2005) Three genomes differentially contribute to the biosynthesis of benzoxazinones in hexaploid wheat. *Proc Natl Acad Sci USA* **102**: 16490–16495
- Notebaart RA, Huynen MA, Teusink B, Siezen RJ, Snel B (2005) Correlation between sequence conservation and the genomic context after gene duplication. *Nucleic Acids Res* **33**: 6164–6171
- Ohno S (1970) *Evolution by Gene Duplication*. Springer, New York
- Osborn TC, Pires JC, Birchler JA, Auger DL, Chen ZJ, Lee HS, Comai L, Madlung A, Doerge RW, Colot V, et al (2003) Understanding mechanisms of novel gene expression in polyploids. *Trends Genet* **19**: 141–147
- Paterson AH, Bowers JE, Bruggmann R, Dubchak I, Grimwood J, Gundlach H, Haberer G, Hellsten U, Mitros T, Poliakov A, et al (2009) The Sorghum bicolor genome and the diversification of grasses. *Nature* **457**: 551–556
- Paterson AH, Bowers JE, Chapman BA (2004) Ancient polyploidization predating divergence of the cereals, and its consequences for comparative genomics. *Proc Natl Acad Sci USA* **101**: 9903–9908
- Paterson AH, Bowers JE, Peterson DG, Estill JC, Chapman BA (2003) Structure and evolution of cereal genomes. *Curr Opin Genet Dev* **13**: 644–650
- Pond SL, Frost SD, Muse SV (2005) HyPhy: hypothesis testing using phylogenies. *Bioinformatics* **21**: 676–679
- Pumphrey M, Bai J, Laudencia-Chinguanco D, Anderson O, Gill BS (2009) Nonadditive expression of homoeologous genes is established upon polyploidization in hexaploid wheat. *Genetics* **181**: 1147–1157
- Qi L, Friebe B, Wu J, Gu Y, Qian C, Gill BS (2010) The compact Brachypodium genome conserves centromeric regions of a common ancestor with wheat and rice. *Funct Integr Genomics* **10**: 477–492
- Qi LL, Echalié B, Chao S, Lazo GR, Butler GE, Anderson OD, Akhunov ED, Dvorák J, Linkiewicz AM, Ratnasiri A, et al (2004) A chromosome bin map of 16,000 expressed sequence tag loci and distribution of genes among the three genomes of polyploid wheat. *Genetics* **168**: 701–712
- Reddy ASN (2007) Alternative splicing of pre-messenger RNAs in plants in the genomic era. *Annu Rev Plant Biol* **58**: 267–294
- Roux J, Robinson-Rechavi M (2011) Age-dependent gain of alternative splice forms and biased duplication explain the relation between splicing and duplication. *Genome Res* **21**: 357–363
- Salse J, Bolot S, Throude M, Jouffe V, Piegue B, Quraishi UM, Calcagno T, Cooke R, Delseny M, Feuillet C (2008) Identification and characterization of shared duplications between rice and wheat provide new insight into grass genome evolution. *Plant Cell* **20**: 11–24
- Schnable JC, Springer NM, Freeling M (2011) Differentiation of the maize subgenomes by genome dominance and both ancient and ongoing gene loss. *Proc Natl Acad Sci USA* **108**: 4069–4074
- Schnable PS, Ware D, Fulton RS, Stein JC, Wei F, Pasternak S, Liang C, Zhang J, Fulton L, Graves TA, et al (2009) The B73 maize genome: complexity, diversity, and dynamics. *Science* **326**: 1112–1115
- Severin AJ, Cannon SB, Graham MM, Grant D, Shoemaker RC (2011) Changes in twelve homoeologous genomic regions in soybean following three rounds of polyploidy. *Plant Cell* **23**: 3129–3136
- Soltis DE, Bell CD, Kim S, Soltis PS (2008) Origin and early evolution of angiosperms. *Ann N Y Acad Sci* **1133**: 3–25
- Terashima A, Takumi S (2009) Allopolyploidization reduces alternative splicing efficiency for transcripts of the wheat DREB2 homolog, WDREB2. *Genome* **52**: 100–105
- Van de Peer Y, Maere S, Meyer A (2009) The evolutionary significance of ancient genome duplications. *Nat Rev Genet* **10**: 725–732
- Wang BB, Brendel V (2006) Genomewide comparative analysis of alternative splicing in plants. *Proc Natl Acad Sci USA* **103**: 7175–7180
- Wang W, Zheng H, Fan C, Li J, Shi J, Cai Z, Zhang G, Liu D, Zhang J, Vang S, et al (2006) High rate of chimeric gene origination by retroposition in plant genomes. *Plant Cell* **18**: 1791–1802
- Wicker T, Buchmann JP, Keller B (2010) Patching gaps in plant genomes results in gene movement and erosion of colinearity. *Genome Res* **20**: 1229–1237
- Wicker T, Mayer KF, Gundlach H, Martis M, Steuernagel B, Scholz U, Simková H, Kubaláková M, Choulet F, Taudien S, et al (2011) Frequent gene movement and pseudogene evolution is common to the large and complex genomes of wheat, barley, and their relatives. *Plant Cell* **23**: 1706–1718
- Yang Z (2007) PAML 4: phylogenetic analysis by maximum likelihood. *Mol Biol Evol* **24**: 1586–1591
- Yang Z, Nielsen R (2000) Estimating synonymous and nonsynonymous substitution rates under realistic evolutionary models. *Mol Biol Evol* **17**: 32–43
- Zhang G, Guo G, Hu X, Zhang Y, Li Q, Li R, Zhuang R, Lu Z, He Z, Fang X, et al (2010) Deep RNA sequencing at single base-pair resolution reveals high complexity of the rice transcriptome. *Genome Res* **20**: 646–654
- Zhou R, Moshgabadi N, Adams KL (2011) Extensive changes to alternative splicing patterns following allopolyploidy in natural and resynthesized polyploids. *Proc Natl Acad Sci USA* **108**: 16122–16127
- Zhu Z, Zhang Y, Long M (2009) Extensive structural renovation of retrogenes in the evolution of the Populus genome. *Plant Physiol* **151**: 1943–1951